J Mol Model (2011) 17:555–564
DOI 10.1007/s00894-010-0754-0

ORIGINAL PAPER

Molecular trigger for pre-transfer editing pathway in Valyl-tRNA synthetase: A molecular dynamics simulation study

Li Li · Long Yu · Qiang Huang

Received: 5 April 2010 / Accepted: 11 May 2010 / Published online: 30 May 2010

Abstract Pre-transfer editing pathway in Valyl-tRNA synthetase (ValRS) is a very important process to maintain the high fidelity of protein synthesis. However, molecular basis for this pathway remains unclear. Here we employed molecular dynamics (MD) simulation to study two complexes, ValRS·tRNA^{val}·Val-AMP (complex V) and ValRS·tRNA^{val}·Thr-AMP (complex T), and compared their simulation trajectories, in order to understand how the pre-transfer editing pathway is triggered by the noncognate substrate Thr-AMP. The MD simulations showed that the binding of Thr-AMP to ValRS led to different motions from those in complex V: clockwise rotation of the editing domain along the hinge region, and strong motions in the catalytic domain, especially in KMSKS loop. We found that the changed motion of Trp495 induced by Thr-AMP serves as a signal to discriminate Thr-AMP from Val-AMP, and the rigid ^{491}ILFL^{494} segment then propagates this signal from Trp495 to Asp490 and induces dissociation of the salt-bridge Asp490-Arg346 and formation of the salt-bridge Glu189-Lys533. The change in salt-bridges alters the motion of KMSKS loop and the editing domain, and eventually triggers the pre-transfer editing pathway. This study provides a model for the molecular trigger of the pre-transfer editing pathway in ValRS, and is useful for further exploring this process.

L. Li · L. Yu · Q. Huang (✉)
State Key Laboratory of Genetic Engineering,
School of Life Sciences, Fudan University,
Shanghai 200433, China
e-mail: huangqiang@fudan.edu.cn

Present Address:
L. Li
Center of Biophysics and Computational Biology,
University of Illinois at Urbana-Champaign,
Urbana, IL 61801, USA

Keywords Aminoacyl-tRNA synthetases · Editing reaction · Molecular dynamics · Pre-transfer editing pathway · Valyl-tRNA synthetase

Introduction

Aminoacyl-tRNA synthetases (aaRSs) play important roles in maintaining the high fidelity of protein synthesis [1, 2]. They charged the amino acid to the cognate tRNA by a two-step mechanism: in the first step, the amino acid is activated to adenylate at the expense of one ATP; in the second step, the aminoacyl moiety is transferred to tRNA, forming aminoacyl-tRNA [1]. Correct recognition of the substrate is vital to this process, since misactivated aminoacyl-tRNA will cause errors in translation, which may lead to severe diseases [3]. Theoretical study has demonstrated that the discrimination ratio between two amino acids that differ only by one methyl group is about one fifth [4], which is more than 500 times larger than the error rate observed in protein synthesis [5]. Also, it was found that many aaRSs use editing function to hydrolyze the misactivated product. Two different editing pathways have been established: in pre-transfer editing pathway, the misactivated aminoacyl-adenylate is hydrolyzed; and in the post-transfer editing pathway, the mischarged aminoacyl-tRNA is hydrolyzed [6] (Fig. 1a).

Valyl-tRNA synthetase (ValRS), isoleucyl-tRNA synthetase (IleRS), leucyl-tRNA synthetase (LeuRS) are three homologous enzymes belong to the Class Ia aaRSs [7], and rely on editing function to maintain the fidelity. Mutational and crystallographic analyses have shown that the active sites of the post-transfer editing pathway in these three enzymes are all located in the CP1 (connect peptide 1) domain (the editing domain) [8–11]. However, the mech-

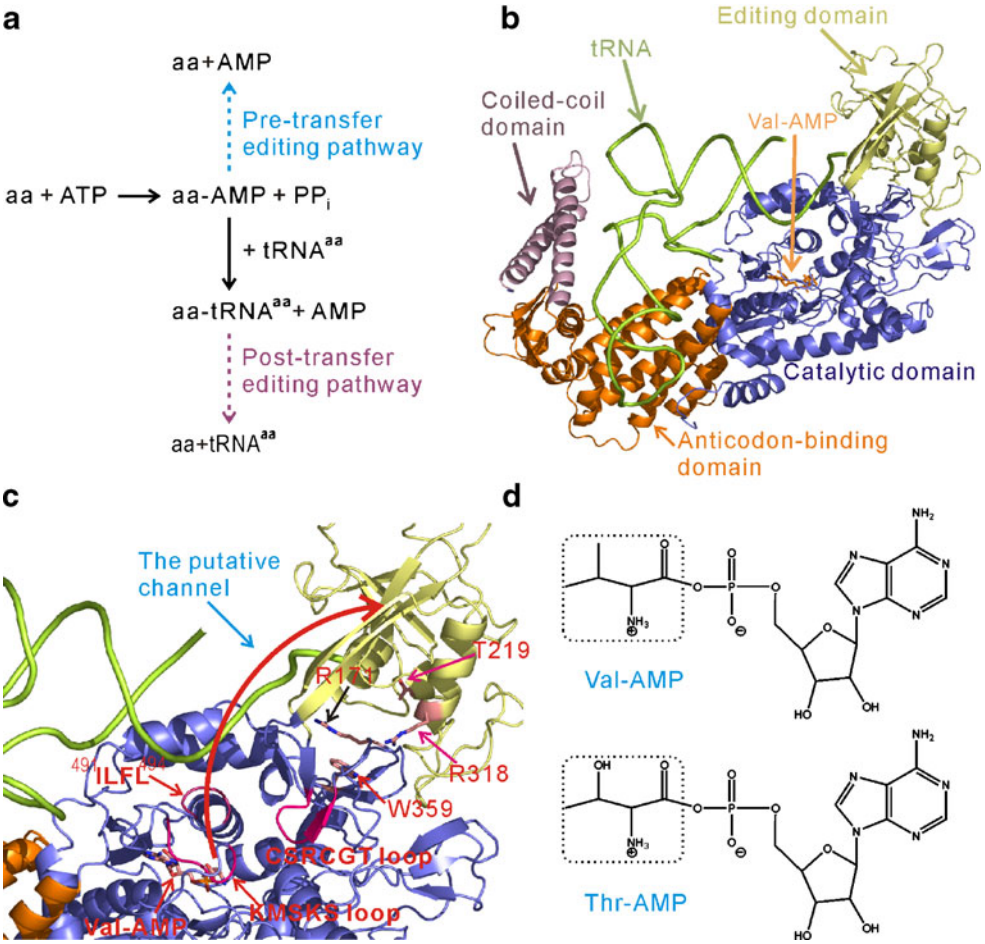

Fig. 1 Enzymatic reactions and editing pathways of aaRSs. (**a**) Aminoacylation and editing reactions of aaRSs. The solid and dot arrows represent aminoacylation and editing reactions, respectively. Amino acid and inorganic pyrophosphate are indicated by aa and PPi, respectively. (**b**) The structure of ValRS·tRNA^{val}·Val-AMS (PDB code: 1GAX), where tRNA is shown as the backbone worm model in green, functional domains of ValRS are showed as the color ribbon models. (**c**) The putative channel for editing in ValRS. The channel is indicated by the red arrow, those identified residues are shown as the stick model in pink, and KMSKS loop, CSRCGT loop and the ^{491}ILFL^{494} segment are shown in red. (**d**) Molecular structures of the substrate Val-AMP and the noncognate substrate Thr-AMP of ValRS

anism and the active site of the pre-transfer editing pathway are controversial. Two different themes have been proposed. In the first scenario, the noncognate adenylate is transported from the aminoacylation site to the CP1 domain, and hydrolyzed in the editing site. This mechanism was supported by the fact that mutating some residues in CP1 domain can abolish the pre-transfer editing activity [10, 11]. Structural analyses were also consistent with this model. For example, based on the crystal structure of IleRS:tRNA complex, Silivan et al. predicted that a channel spanning these two domains might be implicated in the transport [12]. It was further shown by Fukai et al. that the movement of KMSKS loop was critical for opening the channel [13] (Fig. 1b and c). However, this model was challenged by a recent work, which showed that the E. coli LeuRS can still perform pre-transfer editing without the CP1 domain [14] (the ΔCP1 mutant). This work raised an alternative mechanism for the pre-transfer editing pathway: the noncognate adenylate could be first ejected into the solvent and hydrolyzed (the second scenario). However, there is no further evidence to support this model. It is worth pointing out that the second model might be a special case for the first model for the ΔCP1 mutant, i.e., the ejection of the adenylate to the solvent utilizes the same channel as the first model. These taken together, it seems that the transport of the misactivated adenylate is a general feature required for the pre-transfer editing pathway.

A recent study also showed that CP1 domain can bind both pre-and post-editing pathway substrates [15]. However, although tremendous effort has been invested in the understanding of the pre-transfer editing pathway, the molecular basis for the substrate recognition and the driving force of the substrate transport remain unclear. Here, we employed molecular dynamics (MD) simulation to study two complexes: ValRS·tRNA^{val}·Val-AMP and ValRS·tRNA^{val}·Thr-AMP. By comparing their simulation trajectories, we not only verified the previous conclusions about the KMSKS loop [13], but also revealed characteristic motions that might be important for triggering the pre-transfer editing pathway. Such motions were found to be controlled by four salt-bridges and initiated by Trp495, which is adjacent to the substrate in the catalytic domain. We found that the induced motion of Trp495 by Thr-AMP serves as a signal to discriminate the noncognate substrate Thr-AMP from Val-AMP, and the rigid ^{491}ILFL^{494} segment could propagates this motion signal to Asp490 and eventually affect the formation of the identified salt-bridges.

Materials and methods

Structural models of the complexes ValRS·tRNA^{val}·Val-AMP and ValRS·tRNA^{val}·Thr-AMP

In this study, we investigated two ValRS complexes: ValRS·tRNA^{val}·Val-AMP and ValRS·tRNA^{val}·Thr-AMP. Hereafter, we designate ValRS·tRNA^{val}·Val-AMP as complex V, and ValRS·tRNA^{val}·Thr-AMP as complex T, respectively. For both complexes, the *Thermus thermophilus* ValRS structure was taken from the Protein Data Bank (PDB code: 1GAX) [13] (Fig. 1b). For complex V, the Val-AMS was mutated into Val-AMP; and for complex T, the Val-AMS was mutated into Thr-AMP (Fig. 1d).

MD simulations

Using the structural models above as the starting structures, two MD simulation systems with explicit solvent representation were constructed for the complexes V and T, respectively. The simulations were carried out using NAMD 2.6 with the standard CHARMM27 force field parameters [16]. Hydrogen atoms were added to the structures by the program psfgen in NAMD. Thus, in each system, the protein and tRNA contain about 14,000 and 2,400 atoms, respectively. Certain numbers of Na^+ and Cl^- ions were placed around the complexes to mimic the physiological ion concentration of 150 mM and to ensure the neutrality of the simulation systems. TIP3P water molecules were placed around the given complex to form a rectangular box, with a distance not less than 9 Å from the box boundaries to the surface of the simulated complexes. Thus, both simulation systems contain about 4.7×10^4 water molecules, with box dimensions $102 \times 130 \times 126$ Å^3. Periodic boundary conditions with constant temperature and pressure were used. Temperature was kept at 300 K by coupling to an external heat bath using the Berendsen algorithm [17]. Pressure was kept at 1 atm by isotropic scaling using a Berendsen barostat. Particle Mesh Ewald with cubic spline approximation was used to treat long-range electrostatics [18]. The SHAKE algorithm was used to constrain covalent bonds to hydrogen so that a time step of 2 fs could be used [19]. The entire system was first equilibrated and then atomic coordinates were saved every 2 ps for analysis. Simulation periods for both systems were 10 ns. Simulations were carried out on the Shenteng-1800 Cluster Computer with 32 Intel Xenon 2.8 GHz CPUs in our laboratory.

Trajectory analysis

The MD atomic fluctuations of residues were calculated by the PTRAJ module of AMBER [20]. The cross-correlation analysis was performed by homemade MATLAB programs using the method described in Estabrook et al. [21]. To extract the dominant modes of motions in two simulated complexes, principal component analysis (PCA) was conducted by the online program DYNAMITE (http://dynamite.biop.ox.ac.uk/dynamite) [22]. The direction and amplitude of a given dynamic mode was represented by its eigenvector and eigenvalue, respectively. As in our previous study [23], to avoid exceeding the memory capacity of computer, only C_α atoms were considered in the analysis.

3D viewers of molecular structures

The programs VMD [24] and PyMOL (http://www.pymol.org) were used to create images of the protein structures in all figures, including the porcupine plots for the principal dynamic modes obtained by PCA .

Results and discussion

Biological implication of the ValRS·tRNA^{val}·Val-AMS complex structure

To conduct the MD simulations for complex V (ValRS·tRNA^{val}·Val-AMP) and complex T (ValRS·tRNA^{val}·Thr-AMP), we constructed the initial MD structures for the complexes based on the crystal structure of ValRS·tRNA^{val}·Val-AMS (PDB code: 1GAX) [13] (see Materials and methods). So it is important to clarify why the models based on 1GAX are appropriate for studying the pre-transfer editing pathway in the ValRS. Although originally Fukai et al. suggested that 1GAX mimics the conformation of the ValRS complex in the post-transfer editing pathway [13], mainly based on that the A76 nucleotide is located in the editing domain, newly emerged results implied that 1GAX resembles a conformation after the aminoacylation step (see below). The conformation of the acceptor stem in 1GAX could be explained by such a hypothesis: when the ValRS completes their aminoacylation step and begins the aminoacyl-transfer step, the A76 nucleotide end of tRNA needs to go through the editing domain to enter the catalytic site, and 1GAX actually represents a snapshot in this process.

This hypothesis is supported by three facts. First, Rock et al. have elucidated that a certain kind of fungicide abolishes the catalytic activity of LeuRS by trapping the cognate tRNA^{Leu} in the editing domain [25], strongly indicating that the A76 nucleotide needs to pass by the editing domain in LeuRS before it enters the catalytic domain. Due to the high similarity between ValRS and LeuRS, this result is a very strong support. Second, Mursinna et al. have shown that a single mutation in the

editing domain of LeuRS can trigger the hydrolyzation of the cognate Leu-tRNA^{Leu} [26]. This indicates that the A76 nucleotide of the Leu-tRNA^{Leu} would pass by the editing domain when it leaves. Third, Fukai et al. have co-crystallized ValRS with tRNA^{val} and Val-AMS, but not with the post-transfer editing pathway's substrate Thr-tRNA^{Val}. Based on these facts, it is reasonable to deduce that the complex V will perform the aminoacylation reaction and the complex T may either undergo the pre-transfer editing pathway or transfer the threonyl group to the tRNA (aminoacylation). If complex T conducts the aminoacylation reaction, the main dynamic features in these two complexes should be almost the same; while in the other case, they should be very different [13]. Thus, by comparing the dynamic features of these two complexes, one could find out the actual reaction that the ValRS performs.

Atomic fluctuations in the editing domain of complex V is substantially larger than those in complex T

As mentioned in Materials and methods, the MD simulation periods for both complexes were 10 ns. The root mean square deviations (RMSDs) of backbone heavy atoms of the proteins shown in Fig. 2a demonstrate that the MD simulations have been equilibrated when the first 3-ns simulation runs were completed. Therefore, the MD trajectories from 3 to 10 ns were used in the following analyses.

To examine the difference in dynamics between two complexes, we first compared the root-mean-square fluctuations (RMSF) of residues for two complexes. The RMSF of a given residue in the MD trajectories were calculated by averaging over all the atoms of the given residue, and are shown in Fig. 2b. In the figure, we can see that the RMSFs of the editing domain in complex V (amino acids from 192 to 340) is substantially larger than those in complex T, while other residues in these two complexes are similar. The observed large atomic fluctuations in the editing domain of the complex V is consistent with previous crystallographic results [13], and indicates that the editing domain experiences large conformational changes in the aminoacyl-transfer reaction. In contrast, the relatively small fluctuations in the editing domain of complex T imply that the binding of the noncognate substrate Thr-AMP might trigger a new reaction different from the aminoacyl-transfer reaction.

If the complex V is in the aminoacyl-transfer state, one may expect to observe the translocation of the CCA end of tRNA from the editing site to the aminoacylation site. However, such kind of large movement is unlikely to be observed in the 10-ns simulations. In our simulations, the CCA end of tRNA kept bound to the editing domain in both complexes. Thus, to study the large movement of the CCA end, millisecond-scale or longer simulations seem to be required.

Movement of the editing domain of complex V is consistent with Fukai's model

The RMSF results have shown that the dynamics in two complexes are very different. To better understand such differences, we first combined cross-correlation analysis and principal component analysis (PCA) to examine the MD trajectories of complex V.

In the cross-correlation analysis, we calculated the cross-correlation coefficients $C(i, j)$ between all the residues/nucleotides to characterize the correlated motions between different parts in the complexes. Residue pairs with positive $C(i, j)$ move in the same direction and are designed as correlated residues, whereas residues with negative $C(i, j)$ move in the opposite directions and designed as anti-correlated residues. A completely correlated or anti-correlated motion, $C(i, j) = 1$ or $C(i, j) = -1$, means that the motions have the same phase and period. The matrix of the cross-correlation coefficients for the C_α atoms of ValRS is shown in Fig. 2c, where the amino-acids of different domains of ValRS are indicated in the color bar above the matrix. As expected, the motions within the catalytic domain are highly coupled, indicating that the residues of the active site move collectively to accommodate the cognate substrate Val-AMP. In addition, the editing domain exhibits a strong anti-correlated motion against the rest part of ValRS, which is consistent with Fukai's model [13].

To investigate the movement direction of the editing domain, we employed PCA to extract the dynamic modes of the protein complexes in the simulation. PCA describes the motions of the atoms in a protein in terms of a small number of dynamic modes, and the eigenvectors and eigenvalues of the modes highlight direction and the amplitude of dominant modes of protein motion [22, 27]. The normalized eigenvalues show that the first dynamic mode in complex V is principal (~57% in Fig. 2e). This dominant dynamic mode is represented by the porcupine plots in Fig. 3a and c. The figures show that, the catalytic domain moves as a rigid body with very small amplitude and the editing domain rotates anticlockwise along the hinge region significantly, consistent with the cross-correlation analysis (see also Fig. 1b). Significantly, the movement direction of the editing domain is also consistent with Fukai's model.

Binding of Thr-AMP alters the motions of the KMSKS loop and the editing domain

The cross-correlation analysis and PCA have revealed the characteristic motions of the editing domain in complex V.

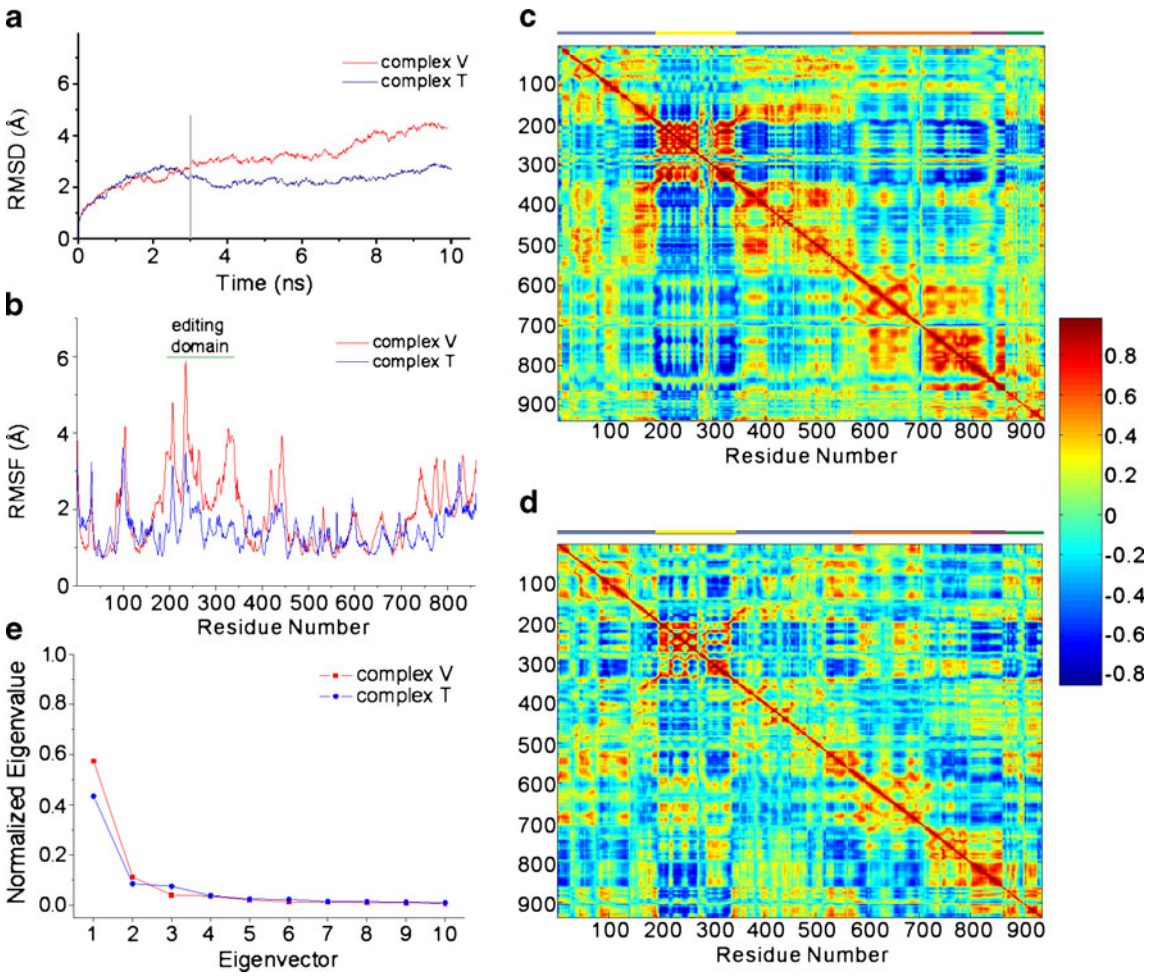

Fig. 2 Molecular motions of complex V and complex T. (**a**) RMSDs of backbone heavy atoms of the proteins in complexes V (red) and T (blue), where the MD starting structures were the references. (**b**) RMSFs of residues in complexes V (red) and T (blue). (**c**) The cross-correlation matrix for motions of the C_α atoms in ValRS (indicated by numbers 1–863) and the center-of-mass of all nucleotides in the tRNA (indicated by numbers 864–939) in complex V. The correlations were calculated after superimposing each snapshot structure in the trajectories onto the first structure. The scale of the correlations is indicated on the spectrum on the right, and the color bar above indicates the domains that the residues belong to (catalytic domain, blue; editing domain, yellow; anticodon-binding domain, orange; coiled-coil domain, purple; tRNA, green). (**d**) The cross-correlation matrix for complex T. (**e**) Dominant dynamic modes in complex V and complex T. Relative contributions of different modes (eigenvectors) to the overall motion are shown for complex V (red) and complex T (blue), respectively. The data were renormalized so that the eigenvalues for each set add up to unity

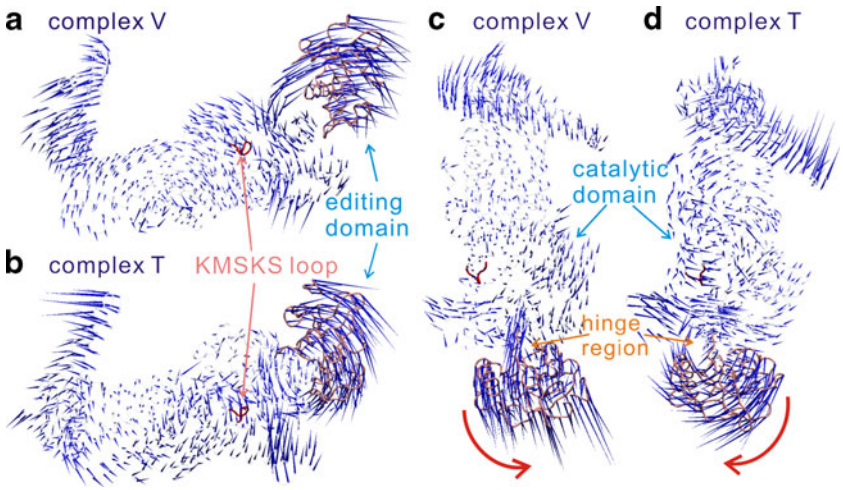

Fig. 3 Principal dynamic modes in complex V and complex T represented by porcupine plots. (**a**) The side view of complex V. (**b**) The side view of complex T. (**c**) The perpendicular view of complex V. The red arrow shows the anticlockwise direction of editing domain's motion along the hinge region. (**d**) The perpendicular view of complex T. The red arrow shows the clockwise direction of editing domain's motion along the hinge region, which is opposite to that in complex V

Thus, we used the same approaches to analyze the MD trajectories of complex T, in order to understand the dynamic features when the noncognate substrate Thr-AMP binds to ValRS.

Compared to complex V, the dynamics of ValRS binding to Thr-AMP alters significantly (Figs. 2d, 3b and d). For example, the cross-correlation analysis showed that the correlated motions in the catalytic domain of complex T are greatly decreased (Fig. 2d). The PCA showed that there exists also a dominant dynamic mode in complex T (Fig. 2e), and the change in the catalytic domain is also observed in this mode (Fig. 3b and d). Moreover, PCA showed that the KMSKS loop (amino acids from 528 to 533) and the nearby CSRCGT loop (amino acids from 344–-349) undergo large movements and the movement directions are consistent with Fukai's model (see also Fig. 1c for the positions of two loops). Such large movements might be responsible for the opening of the channel. Also, from the porcupine plots, we can see that the movements of the catalytic domain are strong, and the editing domain rotates clockwise rather than anticlockwise along the hinge region (Fig. 3b and d).

Combining the results in the previous three subsections, we may conclude that the dynamics in complexes V and T are significantly different. Very likely, the binding of Thr-AMP to ValRS leads to characteristic dynamics required for the pre-transfer editing pathway. And two features in dynamics might be important for the pathway: (i) the clockwise rotation of the editing domain, (ii) the strong movements in the catalytic domain, especially the KMSKS loop and the CSRCGT loop.

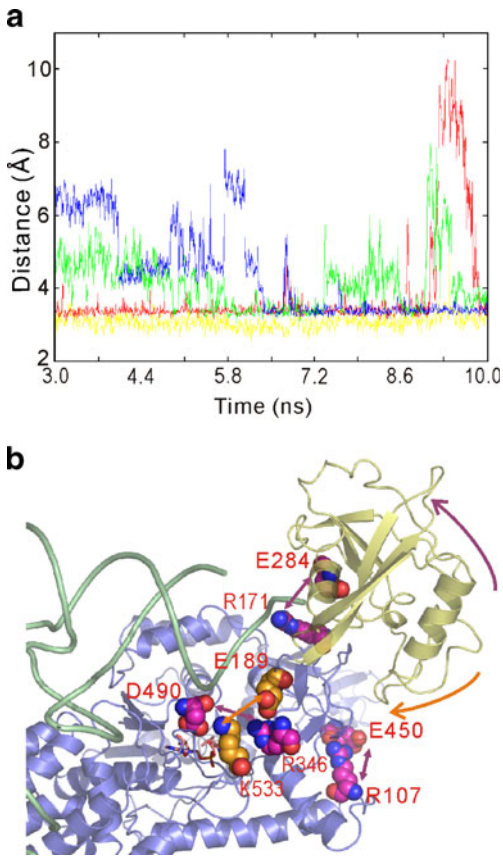

Fig. 4 The salt-bridges that are suggested control the motion of editing domain. (**a**) MD snapshots of the distances between the O, N atoms in the following salt-bridges: Glu189-Lys533 in complex T (yellow), Glu284-Arg171 in complex V (red), Glu450-Arg107 in complex V (green), Asp490-Arg346 in complex V (blue). The snapshots were extracted from the MD trajectories from 3 to 10 ns. (**b**) The salt-bridge in complex T (orange) facilitates the clockwise rotation of the editing domain (indicated by the orange arrow), while the salt-bridges in complex V (pink) enhance the anti-clockwise rotation of editing domain (indicated by the pink arrow)

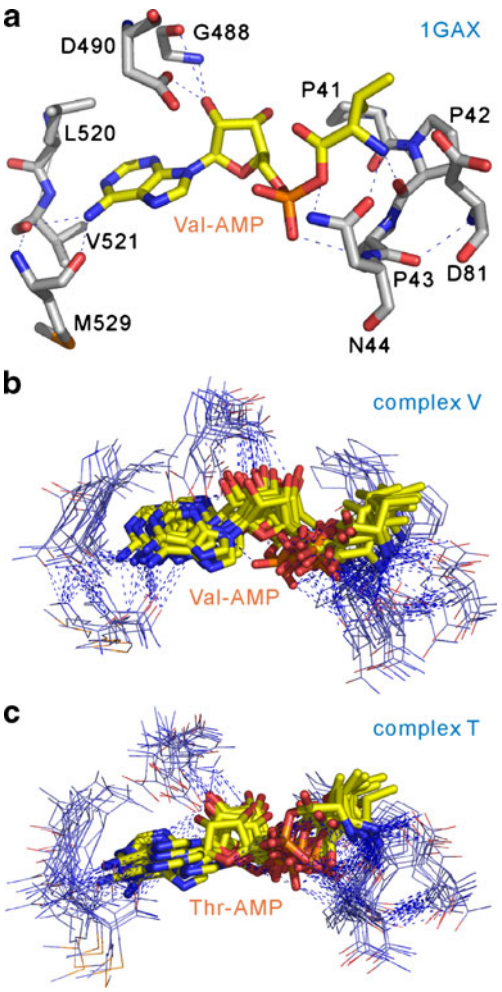

Fig. 5 Similar binding modes of different substrates to ValRS. (**a**) The molecular interactions between the substrate (Val-AMS has been mutated into Val-AMP) and the ValRS in crystal structure (PDB code: 1GAX). (**b**) Seven superimposed MD snapshots (at 4, 5, 6, 7, 8, 9, and 10 ns, respectively) show that the Val-AMP (stick model) in complex V interacts with ValRS similarly as compared to the crystal structure. (**c**) Seven superimposed MD snapshots (at 4, 5, 6, 7, 8, 9, and 10 ns, respectively) show that the Thr-AMP (stick model) in complex T interacts with ValRS similarly as compared to the complex V

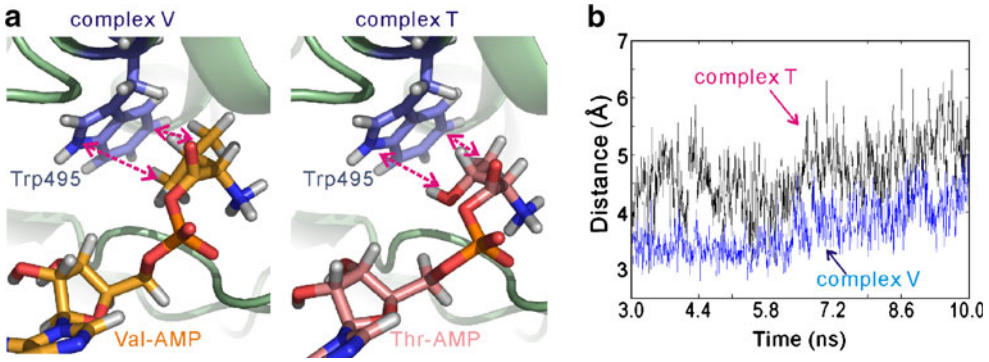

Fig. 6 Trp495 discriminates Thr-AMP from Val-AMP. (**a**) In complex V (left) and complex T (right), Trp495 interacts with Val-AMP (yellow) and Thr-AMP (pink) directly. (**b**) MD snapshots of selected distances during the MD simulations from 3 to 10 ns. The black curve shows the distance between the hydroxyl group in the threonyl of Thr-AMP and the N atom in the indole ring of Trp495, and the blue curve shows the distance between the methyl group in the valyl of Val-AMP and the N atom in the indole ring of Trp495

The motions of the KMSKS loop and the editing domain are controlled by salt-bridges

Why the motions in complexes V and T are so different? To address this, we turned to unravel the residues that control these movements by examining the MD trajectories of two complexes. We carefully examined the formation of salt-bridges in complexes V and T. Very interestingly, we found that, while the majority of salt-bridges remained the same, the substitution of Thr-AMP for Val-AMP does induce the formation of a new salt bridge (Glu189 – Lys533) and dissociate three other salt bridges (Glu284 – Arg171, Glu450 – Arg107, Asp490 – Arg346) (Fig. 4).

There are three important features for those salt-bridges. First, the locations of the salt-bridges strongly correlated with the rotational directions of the editing domain. Glu189-Lys533 is located in the left side of the editing domain, facilitating the clockwise rotation of editing domain; while other three salt-bridges are located in the right side, enhancing the anticlockwise rotation of the editing domain. Second, Glu189-Lys533 and Asp490-Arg346 are both located in the catalytic domain. Change in these two salt-bridges might be responsible for the intense movements of the catalytic domain in complex T. Also, Lys533 is adjacent to the KMSKS loop, and the formation of the Glu189-Lys533 salt-bridge is likely to lead to the large conformational change in the KMSKS loop. Finally, from the three dimensional structures we can see that Glu189-Lys533 and Asp490-Arg346 form a cross, and they might act as a "molecular switch" to determine the reaction that ValRS performs.

Trp495 discriminates Thr-AMP from Val-AMP, and the ^{491}ILFL^{494} segment propagates the discrimination signal

We further identified the residues that discriminate the noncognate substrate Thr-AMP from Val-AMP and lead to the different characteristic motions in complexes V and T. In the MD simulations, Val-AMP and Thr-AMP were found to bind to the active site in a very similar way (Fig. 5). So it is very unlikely that the change in salt-bridges is induced by the different substrate binding patterns. Then, we focused on the residues that are close to the discriminating methyl/hydroxyl group. We found that the rigid indole ring of Trp495 interacts directly with this methyl/hydroxyl group and this residue could be considered as the best candidate. Figure 6 shows the MD snapshots of the distances between the nitrogen atom in the indole ring of Trp495 and the methyl/hydroxyl group in two complexes, which were extracted from the MD simulation trajectories from 3 to 10 ns. The average distance between Trp495 and Val-AMP is 4.18 Å, which is about 1 Å shorter than that between Trp495 and Thr-AMP (5.17 Å). The longer distance between Trp-AMP and Trp495 is induced by the repulsive electrostatic interactions between the hydroxyl of Thr-AMP and Trp495. Likely, such an enlarged distance induced by Thr-AMP is the major factor to discriminate Thr-AMP from Val-AMP.

Now, we focus on elucidating the signal transduction pathway from Trp495 to those salt-bridges. We found that the ^{491}ILFL^{494} segment links Trp495 to Asp490 directly, and the highly correlated values obtained by the cross-correlation analysis indicates that this segment is very rigid (Table 1, see also Fig. 1c for the position of the he

Table 1 Cross-correlation coefficients of the segment ^{491}ILFL^{494} in MD simulations

Residue	491	492	493	494
491	1.00			
492	0.82	1.00		
493	0.44	0.71	1.00	
494	0.42	0.58	0.89	1.00

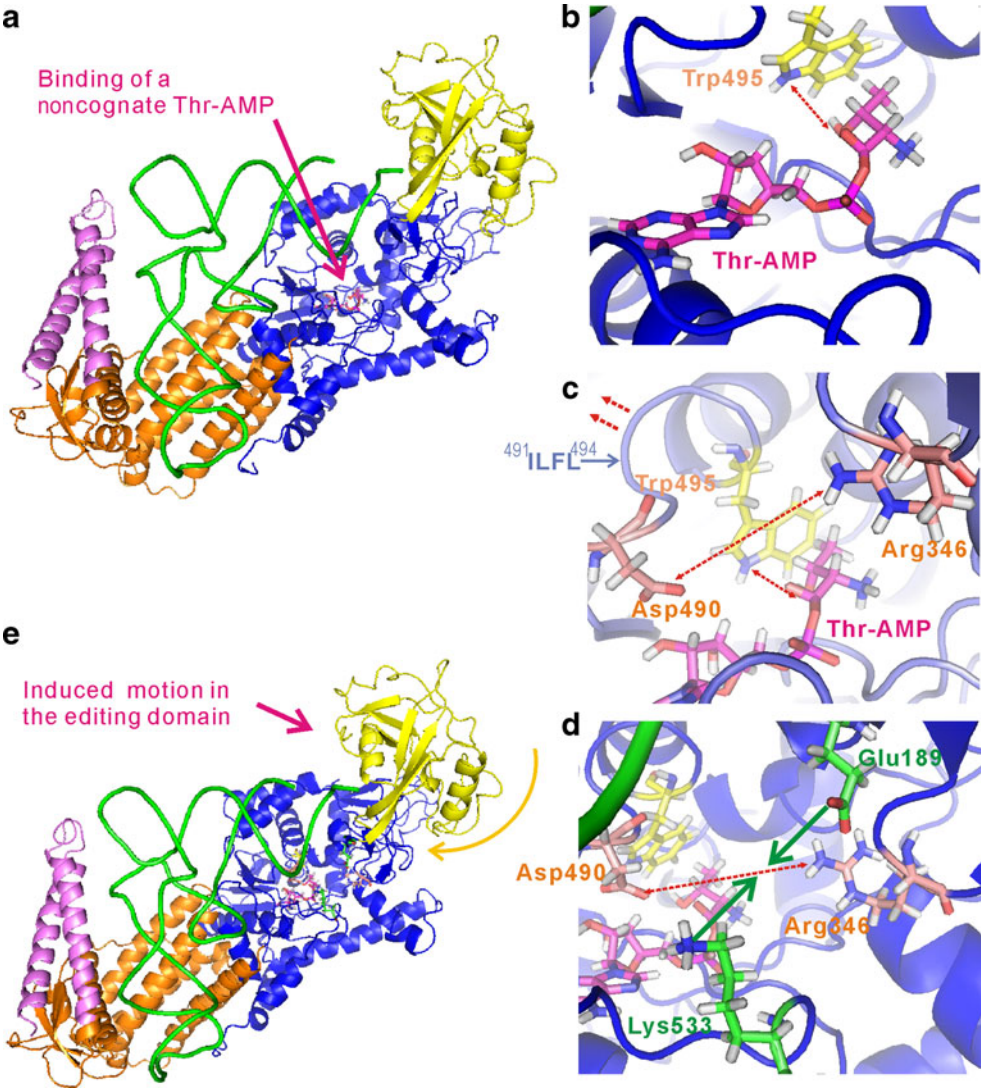

Fig. 7 A molecular model for the pre-transfer editing pathway in ValRS. The signal of a non-cognate Thr-AMP binding (**a**) is first recognized by Trp495 (**b**), this signal is further amplified by the movement of Asp490, and thereby enhances the formation of the Asp490-Arg346 salt-bridge (**c**) and weakens the Glu189-Lys533 salt bridge (**d**). This finally triggers the clockwise motion of the editing domain (e, yellow arrow) and the pre-transfer editing pathway in ValRS

^{491}ILFL^{494} segment). The distance change of about 1 Å in Trp495 may be amplified by this segment, and thereby the distance between Asp490 and Arg346 is also enlarged. This leads to the dissociation of the salt-bridge Asp490-Arg346, and consequently triggers the formation of a new salt-bridge: Glu189-Lys533. Thus, it appears that this rigid segment ^{491}ILFL^{494} might be responsible for propagating the induced motion signal from Trp495 to the salt-bridges (Asp490), and eventually trigger the characteristic motions in complex T different from those in complex V.

A model for the molecular trigger of the pre-transfer editing pathway in ValRS

Based on above results, we postulated a model for the molecular trigger of the pre-transfer editing pathway in ValRS: the noncognate substrate Thr-AMP is first recognized by Trp495, and this enlarges the distance between Thr-AMP and Trp495 (about 1 Å larger than Val-AMP); this motion signal is further amplified by the rigid ^{491}ILFL^{494} segment and propagated to Asp490; then the distance between Arg346 and Asp490 is increased and thereby the salt-bridge Asp490-Arg346 is broken, and a new salt-bridge Glu189-Lys533 is formed; the change in salt-bridges in the catalytic domain alters the motions of the

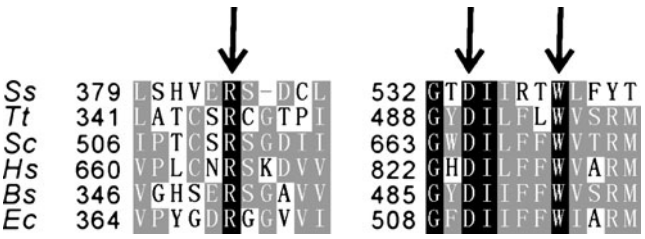

Fig. 8 Multiple sequence alignment of ValRS sequences from six species (*Sulfolobus solfataricus*, Ss; *Thermus thermophilus, Tt*; *Saccharomyces cerevisiae, Sc*; *Homo sapiens, Hs*; *Bacillus subtilis, Bs*; *Escherichia coli, Ec*). Detailed analysis on sequence conservation of ValRS and LeuRS can also be seen in Ref. 29

KMSKS loop and the editing domain, and eventually triggers the pre-transfer editing pathway in ValRS (Fig. 7).

Several experimental results corroborate our model. First of all, in our simulations, we observed a large movement of the KMSKS loop, which is consistent with Fukai's structural study [13] that showed movement of the KMSKS loop is critical for pre-transfer editing pathway. Secondly, our PCA revealed the direction of the editing domain's movement in pre-transfer editing pathway, which is also supported by Fukai's results of structural alignment [13]. Finally, our theoretical work explains why mutations A293D and K186E in *E. coli* LeuRS can rescue the pre-transfer editing activity. These mutations can facilitate the rotation of the editing domain toward the pre-transfer editing state by means of electrostatic interactions [28].

Our model also gains supports from evolutionary analysis [29]. Multiple sequence alignment of ValRS sequences from six species (*Sulfolobus solfataricus*, *Thermus thermophilus*, *Saccharomyces cerevisiae*, *Homo sapiens*, *Bacillus subtilis*, *Escherichia coli*) showed that Trp495 is highly conserved in evolution (Fig. 8), strongly indicating that Trp495 plays an important role in maintaining the functions of ValRS. In our model, Trp495 was suggested to discriminate the noncognate Thr-AMP from the cognate Val-AMP, and this might explain why Trp495 is so conserved. Meanwhile, the salt-bridges identified in above (*e.g.*, Asp490-Arg346) were also found to be rather conserved.

Compared to Fukai's model, our results not only showed the importance of the KMSKS loop in the pre-transfer editing pathway, but also revealed several dynamic features that might be required for the pre-transfer editing pathway, *e.g.*, the anticlockwise rotation of the editing domain. Also, we elucidated the driving force for the large conformational change and the putative transduction pathway of discriminating signal. The identified salt-bridges and the discriminating residue Trp495 can serve as starting points for further experiments to explore the pre-transfer editing pathway in ValRS.

Conclusions

In this study, we have investigated two complexes, ValRS·tRNA^{val}·Val-AMP (complex V) and ValRS·tRNA^{val}·Thr-AMP (complex T) by MD simulation, in order to unravel the molecular trigger for the pre-transfer editing pathway in ValRS. By comparing the nanosecond-scale simulation trajectories of two complexes, we found that the atomic fluctuations in the editing domain of complex V are significantly larger than those in complex T, and the movement of the editing domain in complex V is consistent with Fukai's model [13]. Very importantly, we found that the binding of the noncognate substrate Thr-AMP to ValRS led to different characteristic motions, such as the clockwise rotation of the editing domain, and strong movements in the catalytic domain, especially in the KMSKS loop and the CSRCGT loop. We found that the binding of the noncognate substrate Thr-AMP is firstly recognized by Trp495, and the induced motion signal of Trp495 is then propagated by the rigid ^{491}ILFL^{494} segment from Trp495 to Asp490 and thereby triggers the dissociation of the salt-bridge Asp490-Arg346 and the formation of a new salt-bridge Glu189-Lys533. The change in these salt-bridges alters the motions of the KMSKS loop and the editing domain, and eventually initiates the pre-transfer editing pathway in ValRS. Thus, this study provides a model for the molecular trigger of the pre-transfer editing pathway in ValRS, which may shed light on the pre-transfer editing mechanism and is useful for further exploring this process.

Acknowledgments This study was supported in part by the National Natural Science Foundation of China (Grant No. 30570406), the HI-tech Research and Development Program of China (Grant No. 2008AA02Z311), and Shanghai Supercomputer Center of China.

References

1. Ibba M, Söll D (2000) Annu Rev Biochem 69:617–650
2. Ibba M, Söll D (1999) Science 286:1893–1897
3. Lee JW, Beebe K, Nangle LA, Jang J, Longo-Guess CM, Cook SA, Davisson MT, Sundberg JP, Schimmel P, Ackerman SL (2006) Nature 443:50–55
4. Pauling L (1957) The probability of errors in the processes of synthesis of protein molecules. Festschrift für Prof Dr Arthur Stoll zum siebzigsten Geburtstag. Birkhäuse, Basel, In, pp 597–602
5. Loftfield RB (1963) Biochem J 89:82–92
6. Jakubowski H, Goldman E (1992) Microbiol Rev 56:412–429
7. Arnez JG, Moras D (1997) Trends Biochem Sci 22:211–216
8. Nureki O, Vassylyev DG, Tateno M, Shimada A, Nakama T, Fukai S, Konno M, Hendrickson TL, Schimmel P, Yokoyama S (1998) Science 280:578–582
9. Lin L, Hale S, Schimmel P (1996) Nature 384:33–34
10. Hendrickson T, Nomanbhoy T, de Crecy-Lagard V, Fukai S, Nureki O, Yokoyama S, Schimmel P (2002) Mol Cell 9:353–362
11. Lincecum TL Jr, Yaremchuk A, Mursinna RS, Williams AM, Sproat BS, Eynde WVD, Link A, Calenbergh SV, Grøtli M, Martinis SA, Cusack S (2003) Mol Cell 11:951–963
12. Silvian LF, Wang J, Steitz TA (1999) Science 285:1074–1077
13. Fukai S, Nureki O, Sekine SI, Shimada A, Tao J, Vassylyev DG, Yokoyama S (2000) Cell 103:793–803
14. Boniecki MT, Vu MT, Betha AK, Martinis SA (2008) Proc Natl Acad Sci USA 105:19223–19228
15. Bharatham N, Bharatham K, Leea Y, Lee KW (2009) Biophys Chem 143:34–43
16. Feller SE, MacKerell AD (2000) J Phys Chem B 104:7510–7515
17. Berendsen HJC, Postma JPM, van Gunsteren WF, Dinola A, Haak JR (1984) J Chem Phys 81:3684–3690
18. Essmann U, Perera L, Berkowitz ML, Darden T, Lee H, Pedersen LG (1995) J Chem Phys 103:8577–8593
19. Ryckaert J, Ciccotti G, Berendsen H (1977) J Comput Phys 23:327–341

20. Case D, Pearlman DA, Caldwell JW, Cheathum TE, Ross WS, Simmerling C, Darden T, Merz KM, Stanton RV, Cheng A, Vincent JJ, Crowley M, Ferguson BM, Radmen R, Seibel GL, Singh UC, Weiner P, Kollman P (1997) AMBER 5.0. University of California, San Francisco, CA
21. Estabrook RA, Luo J, Purdy MM, Sharma V, Weakliem P, Bruice TC, Reich NO (2005) Proc Natl Acad Sci USA 102:994–999
22. Barrett CP, Noble MEM (2005) J Biol Chem 280:13993–14005
23. Shen H, Xu F, Hu H, Wang F, Wu Q, Huang Q, Wang H (2008) J Struct Biol 164:281–292
24. Humphrey W, Dalke A, Schulten K (1996) J Mol Graph 14:33–38
25. Rock FL, Mao W, Yaremchuk A, Tukalo M, Crepin T, Zhou H, Zhang YK, Hernandez V, Akama T, Baker SJ, Plattner JJ, Shapiro L, Martinis SA, Benkovic SJ, Cusack S, Alley MRK (2007) Science 316:1759–1761
26. Mursinna RS, Tommie L, Lincecum J, Martinis SA (2001) Biochemistry 40:5376–5381
27. Brooks BR, Janezi D, Karplus M (1995) J Comput Chem 16:1522–1542
28. Williams AM, Martinis SA (2006) Proc Natl Acad Sci USA 103:3586–3591
29. O'Donoghue P, Luthey-Schulten Z (2003) Microbiol Mol Biol Rev 67:550–573